NASA Technical Paper 2907

1989

A Closed-Form Trim Solution Yielding Minimum Trim Drag for Airplanes With Multiple Longitudinal-Control Effectors

Kenneth H. Goodrich,
Steven M. Sliwa,
and Frederick J. Lallman
Langley Research Center
Hampton, Virginia

NASA
National Aeronautics and Space Administration
Office of Management
Scientific and Technical Information Division

Contents

Symbols

b	surface span, ft
C_D	drag coefficient, Drag force/$\bar{q}S$
$C_{D,i}$	induced drag coefficient, Induced drag force/$\bar{q}S$
C_L	aerodynamic lift coefficient, $L/\bar{q}S$
$C_{L,\Gamma}$	induced lift coefficient, Induced lift force/$\bar{q}S$
$C_{m,o}$	zero-lift pitching-moment coefficient, Zero-lift pitching moment/$\bar{q}Sc$
C_T	thrust coefficient, $T/\bar{q}S$
$C_{T,e}$	effective thrust coefficient, $C_T \cos\delta_v + \eta_{\mathrm{TR}} C_T(1 - \cos\delta_v)$
C_{TL}	thrust-loss coefficient, $\mu_{\mathrm{TL}} C_T(1 - \cos\delta_v)$
c	surface chord, ft
D_i	induced drag
E	influence term as defined in equations (3.1.8) and (4.1.10)
e	efficiency factor
H	Hamiltonian (see eq. (2.5.1))
i	incidence angle, rad
k	induced lift parameter
L	aerodynamic lift force, lb
ℓ	horizontal separation between effectors, ft
M	Mach number
n	number of surfaces
P	effective drag penalty
$\bar{q}$	dynamic pressure, lb/ft^2
S	surface area, ft^2
T	thrust force, lb
U_∞	free-stream velocity
V	tail volume coefficient
$\overline{W}$	total lift coefficient of configuration, Weight/$\bar{q}S$
z	vertical separation between effectors, ft
α	angle of attack of body reference line, rad
δ_v	thrust deflection angle, rad or deg
ϵ	average downwash angle at lifting surface, rad
η_{TR}	fraction of thrust recovered
θ	angle between gravitational horizontal and body reference line, rad
λ	Lagrange multiplier
μ_{TL}	fraction of thrust loss, $1 - \eta_{\mathrm{TR}}$

σ	Prandtl coefficient
$\hat{(\ )}$	normalized term, Quantity/Reference quantity

Subscripts:

cg	center of gravity
j	surface j
k	surface k
jk	interaction terms of surfaces j and k
v	jet nozzle
jv	interaction terms of surface j and jet nozzle (see eq. (4.1.10))
1	wing
2	aft horizontal tail
3	canard

Abbreviations:

LOTS	linear optimum trim solution
s.m.	static margin
VLM	vortex-lattice method

Summary

Airplane designs are currently being proposed with a multitude of lifting and control devices. Because of the redundancy in ways to generate moments and forces, there are a variety of strategies for trimming such airplanes. A linear optimum trim solution (LOTS) is derived using a Lagrange formulation. LOTS enables the rapid calculation of the longitudinal load distribution resulting in the minimum trim drag in level, steady state flight for airplanes with a mixture of three or more aerodynamic surfaces and propulsive control effectors. Comparisons of the trim drags obtained using LOTS, a direct, constrained optimization method, and several ad hoc methods are presented for vortex-lattice representations of a three-surface airplane and a two-surface airplane with thrust vectoring. These comparisons show that LOTS accurately predicts the results obtained from the nonlinear optimization and that the optimum methods result in trim-drag reductions up to 80 percent compared with the ad hoc methods.

1. Introduction

In the interest of increased economy, maneuverability, and safety, airplane designers are proposing configurations with more than two lifting surfaces or longitudinal-control effectors. Examples of these configurations are airplanes with three lifting surfaces (e.g., wing, tail, and canard) or two lifting surfaces and thrust vectoring. Such airplanes are capable of generating more forces than are necessary to maintain longitudinal equilibrium and are thus statically indeterminate. The redundant forces and moments present in these configurations may add many desirable capabilities to the airplanes such as attitude and flight path decoupling, increased damage tolerance, and enhanced aerodynamic efficiency. Some of these benefits have been studied by Kendall (1984), Butler (1983), Rokhsaz and Selberg (1985), and Capone and Reubush (1983). With the increased flexibility that these redundant forces provide, the designer faces new challenges not present in conventional designs. One such challenge is that the individual surface lift coefficients or thrust-vector angles are no longer uniquely determined by the conditions of trimmed flight. For example, the wing, horizontal tail, and canard of a three-surface airplane produce three independent lift forces (within aerodynamic limits). To maintain level trimmed flight, two constraints must be satisfied; the lift must equal the weight of the airplane, and the sum of the moments acting on the airplane must be zero. Thus, the number of independent forces exceeds the number of constraints, and hence there is an unlimited number of load distributions that can satisfy the trim constraints. The designer can capitalize on this indeterminateness by selecting the longitudinal load distribution that will satisfy the constraints and maximize or minimize a given performance function. For cruising flight, a logical parameter to minimize is trim drag.

During the design process, one approach for obtaining the load distribution yielding the minimum trim drag for a specific flight condition is to employ nonlinear programming techniques. These numerical methods use multiple iterations to converge on an optimum solution. Typically, a nonlinear optimization routine implemented on a computer passes a load distribution to a cost-function evaluation routine. This evaluation routine returns the value of a cost function, which is usually based on a weighted sum of the deviation from trim and the trim drag as determined for the load distribution. The optimization routine compares the value of the cost function for the current load distribution with values from previous iterations and, based on this comparison, modifies the distribution in an effort to reduce the cost function. This process continues until the optimization routine converges on the load distribution that yields the lowest obtainable cost-function value. Even though this method generally yields the optimum distribution, it has several shortcomings that may make it unsuitable for a number of situations. For a given configuration, selecting the proper weighting terms in the cost function may require a fair amount of experimentation. In addition, such algorithms frequently need operator supervision to ensure that convergence is occurring properly. Finally, the iterative nature of this type of solution does not by itself provide a designer with insight into the physics governing the airplane. To obtain this insight, a potentially lengthy series of parametric design studies should be conducted on a given configuration.

An analytical solution to the optimum trim problem that addresses many of the limitations of the nonlinear optimization approach has been developed and is detailed in this report. The algorithm is referred to as the linear optimum trim solution, or LOTS. LOTS uses a Lagrange formulation to obtain the longitudinal load distribution for a specific flight condition that will minimize a quadratic model of trim drag while satisfying linearized trim constraints. The LOTS algorithm is closed form and computationally efficient, thus making it compatible with a designer's intentions and needs during the conceptual and preliminary design processes. The speed of the method allows timely optimization of the load distribution, whereas the closed-form nature

permits analysis of the influence effects between control effectors. In addition to its applications in airplane design, LOTS may also have applications in wind-tunnel testing and in-flight operations. These potential uses are discussed briefly in this paper.

The accuracy of LOTS is evaluated by comparing the trim drags obtained from its utilization with those obtained through a nonlinear optimization method. LOTS is also compared with procedures that have been proposed as ad hoc methods of trimming redundantly controlled airplanes during preliminary design. These comparisons were conducted using vortex-lattice models of a general aviation class, three-surface airplane and a two-surface, thrust-vectoring, high-performance airplane.

2. Derivation of LOTS

The goal is to develop a closed-form analytical procedure for optimally scheduling the forces generated by the longitudinal-control effectors of a redundantly controlled airplane with respect to trim drag in steady, unaccelerated flight. Equations are presented that model the prime aerodynamic, propulsive, and gravitational effects; and methods for computing each of the relevant aerodynamic and interference terms are either described or referenced. The model includes vertical force and pitching-moment trim equations along with the classical induced drag expression. An approximate form for the propulsive thrust loss due to vectoring of thrust is developed for incorporation into an effective drag function. This drag function combines the effects of aerodynamic drag and the thrust loss due to vectoring into a single term by treating the thrust loss like an equivalent increase in aerodynamic drag. Influence coefficients modeling the aerodynamic interaction of lifting surfaces and thrust vectoring are included in the equations. The equations presented in this paper represent an airplane with any number of aerodynamic surfaces and a single jet-exhaust nozzle. The equations can easily be generalized to include the effects of multiple nozzles, but only at the expense of an increase in the number of terms.

After developing the equations modeling the airplane, it is possible to solve the problem with nonlinear programming techniques using nonlinear constrained optimization. This approach is desirable if the equations have been augmented with experimental data and there is no time limitation for the computationally intensive calculations. An alternative is presented that is consistent with an airplane designer's goals at preliminary design and with the predicted accuracy of the data available at this stage of the design cycle. In this method, the trim equations are linearized and a Lagrange formulation is used to minimize the drag function while satisfying the trim constraints. The mathematical formulation is described in this section and is applied to two specific airplane configurations in sections 3 and 4.

Once an optimum longitudinal distribution of lift along the vehicle has been determined, the surface deflections and thrust deflection angle can be scheduled to generate the specified lift distribution. Equations for estimating the required stabilizer incidence and/or control surface deflections for a given required lift are presented in appendix A.

2.1. Vertical-Trim Equation

In figure 1 the aerodynamic and propulsive force coefficients acting on a multiple-lifting-surface airplane equipped with thrust vectoring in level, steady state flight are shown. The aerodynamic coefficients acting on the fuselage are combined with those of the primary lifting surface (i.e., the wing) to form a wing/body pair that will simply be referred to as the coefficients for the wing. To maintain level, trimmed flight it is necessary for the airplane to maintain constant altitude. This condition will be satisfied if the vertical aerodynamic and propulsive forces balance the gravitational force acting on the airplane. This balance is achieved for an airplane with n aerodynamic surfaces if

$$\sum_{j=1}^{n} \left[\left(C_{L,j} + k_j C_T \delta_v \right) \cos(\alpha - \epsilon_j - \theta) + C_{D,j} \sin(\alpha - \epsilon_j - \theta) \right] \widehat{S}_j + C_T \sin(\delta_v + \theta) - \overline{W} = 0 \qquad (2.1.1)$$

In this and in the following equations, a caret over a variable (e.g., $\widehat{S}$) indicates that this variable has been nondimensionalized by a reference quantity. In this paper, the planform area of the wing is used as the reference area and the mean aerodynamic chord of that surface is used as the reference length. The term $\overline{W}$ is the total lift coefficient of the configuration; for the purposes of this paper in which only equilibrium cruising flight is considered, $\overline{W}$ is approximated by Weight/$\bar{q}S$. The effective lift coefficient of each surface is expressed as the

sum of the lift coefficient of the surface in the absence of thrust-induced effects ($C_{L,j}$) and the change in the lift of the surface due to supercirculation ($k_j C_T \delta_v$). This change due to supercirculation is a result of the jet wake acting to modify the circulation about the surface; this effect can be quite significant for surfaces located in close proximity to a jet wake. More details on supercirculation and its effects can be found in appendix B. The terms α, ϵ, and θ are the angle of attack of the body reference line, the average downwash angle at the lifting surface, and the angle between the gravitational horizontal and the body reference line, respectively. The thrust coefficient C_T is given as $T/\bar{q}S$.

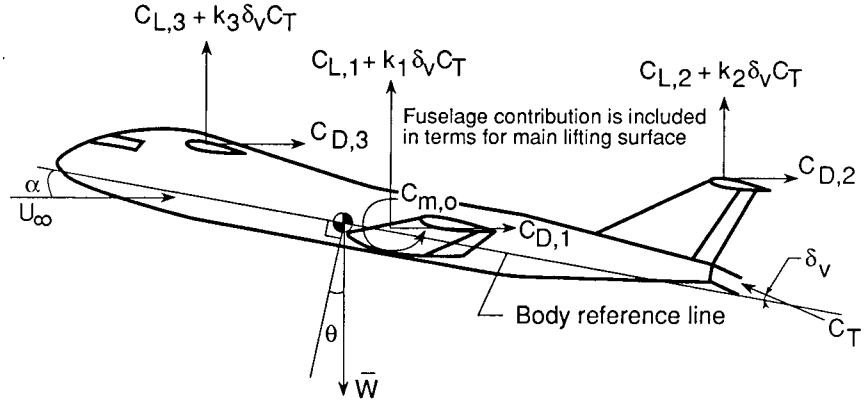

(a) Nondimensionalized forces acting on a multisurface, thrust-vectoring airplane. Fuselage contribution is included in terms for main lifting surface. In equation (2.1.1), the term ϵ_i (not shown here) represents the change in local angle of attack due to downwash.

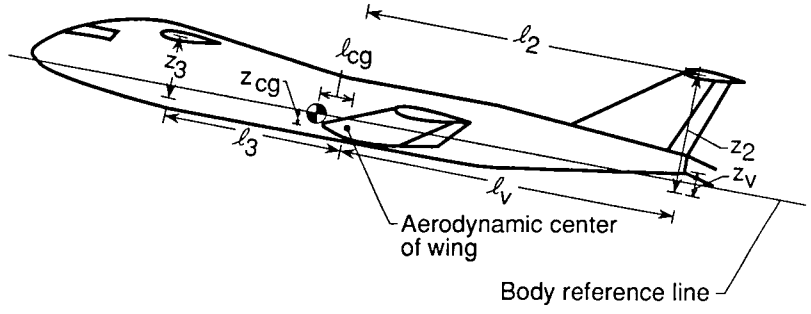

(b) Relevant lengths. All lengths are measured in a body fixed axis system with origin located at aerodynamic center of wing.

Figure 1. Relevant forces and lengths.

The formulation of LOTS requires that the trim equations be linear. Equation (2.1.1) can be linearized when considering cruising flight by making several standard assumptions regarding the relative magnitude and contributions of the drag, thrust, and angular terms. Since this linearization is somewhat configuration-dependent, it will be demonstrated when specific examples are presented in sections 3 and 4.

2.2. Moment-Trim Equation

The moment-trim equation, dictated by the condition that the pitch rate and acceleration be zero, requires the sum of the moments about any point to be zero. If the aerodynamic center of the wing is chosen as the reference point, this condition will be satisfied if the forces and moments are governed by

$$C_{m,o} + \overline{W}\left(\widehat{\ell}_{\mathrm{cg}} \cos\theta + \widehat{z}_{\mathrm{cg}} \sin\theta\right) - C_T\left(\widehat{\ell}_v \sin\delta_v + \widehat{z}_v \cos\delta_v\right) - \sum_{j=2}^{n}\Big\{(C_{L,j} + k_j C_T \delta_v)\left[\cos(\alpha - \epsilon_j)\widehat{\ell}_j + \sin(\alpha - \epsilon_j)\widehat{z}_j\right] + C_{D,j}\left[\cos(\alpha - \epsilon_j)\widehat{z}_j - \sin(\alpha - \epsilon_j)\widehat{\ell}_j\right]\Big\}\widehat{S}_j = 0 \tag{2.2.1}$$

Here, $C_{m,o}$ is the zero-lift pitching moment, $\widehat{\ell}_{\mathrm{cg}}$ and $\widehat{z}_{\mathrm{cg}}$ are the normalized horizontal and vertical separations between the center of gravity and the aerodynamic center of the wing, respectively, $\widehat{\ell}_v$ and $\widehat{z}_v$ are the separations of the exhaust nozzle, and $\widehat{\ell}_j$ and $\widehat{z}_j$ are the separations of the aerodynamic trim surfaces. These separations are measured in the body axis system as indicated in figure 1. Like equation (2.1.1), equation (2.2.1) is easily linearized for cruising flight using common assumptions and will be demonstrated for specific configurations.

2.3. Induced-Drag Equation

Durand (1935) and Butler (1983) express the induced drag of a system of three elliptically loaded lifting surfaces as

$$D_i = \frac{1}{\pi\bar{q}}\left(\frac{\sigma_{11}L_1^2}{e_1 b_1^2} + \frac{\sigma_{22}L_2^2}{e_2 b_2^2} + \frac{\sigma_{33}L_3^2}{e_3 b_3^2} + \frac{2\sigma_{12}}{e_{12}}\frac{L_1 L_2}{b_1 b_2} + \frac{2\sigma_{12}}{e_{12}}\frac{L_1 L_3}{b_1 b_3} + \frac{2\sigma_{23}}{e_{23}}\frac{L_2 L_3}{b_2 b_3}\right) \tag{2.3.1}$$

The subscripts 1, 2, and 3 refer to the wing and two trim surfaces, respectively. The Prandtl coefficients σ_{ij} account for the flow interference between surfaces due to the presence of vortex systems. The efficiency factors e_{ij} account for the effects of viscous flow.

Equation (2.3.1) can easily be extended to analyze systems with any number of lifting surfaces. This extension is accomplished by considering the surfaces in pairs and forming the appropriate influence terms. The resulting equation is most easily expressed in this extended form as a summation. Thus,

$$D_i = \frac{1}{\pi\bar{q}}\sum_{j=1}^{n}\sum_{k=1}^{n}\frac{\sigma_{jk}}{e_{jk}b_j b_k}L_j L_k \tag{2.3.2}$$

where n represents the number of surfaces. For the development of LOTS it is convenient to write the equation in nondimensional form by normalizing the terms by $\bar{q}S_1$. The general induced drag equation can thus be written as

$$C_{D,i} = \sum_{j=1}^{n}\sum_{k=1}^{n}\frac{\sigma_{ik}}{\pi e_{jk}}\frac{S_1}{b_j b_k}\widehat{S}_j\widehat{S}_k(C_{L,j} + k_j\delta_v C_T)(C_{L,k} + k_k\delta_v C_T) \tag{2.3.3}$$

As before, the effective lift coefficient of each surface is separated into a component generated by the free stream and a thrust-induced component.

2.4. Thrust-Loss Expression

When utilizing thrust vectoring to reduce trim drag, some means of accounting for the decrease in the available propulsive force needs to be included. This thrust loss arises from the diversion of propulsive thrust to generate a trim force. For the current study, this effect is accounted for by adding a penalty term to the aerodynamic drag function. This penalty takes the form of the coefficient of thrust loss. Thus,

$$C_{\mathrm{TL}} = \mu_{\mathrm{TL}} C_T(1 - \cos\delta_v) \tag{2.4.1}$$

The $C_T(1 - \cos\delta_v)$ term accounts for propulsive losses from the diversion of thrust from the nominal, undeflected position. The fraction of thrust-loss term μ_{TL} indicates the fraction of this diverted thrust that is not recovered through the process of thrust recovery to provide an effective propulsive force. The thrust-recovery process is a result of favorable interactions between the jet wake and the aerodynamic circulation about the airplane and can significantly reduce the thrust loss associated with thrust vectoring. Experimental data indicate that typical values of μ_{TL} will be between 0 and 0.5 for moderate deflection angles ($\delta_v < 20°$) (Lowry et al. 1957). Additional information on the process of thrust recovery is given in appendix B.

2.5. Lagrangian Formulation

The optimum longitudinal load distribution is defined as the solution to the vertical-trim and moment-trim equations yielding the minimum trim drag. As mentioned in the "Introduction," the rigorous approach to determine this distribution would be to employ nonlinear programming techniques. This approach will result in the solution with the best performance, but, unfortunately, it is often too burdensome to obtain for many applications.

If one is satisfied with the fidelity provided by the quadratic effective-drag model (eq. (2.3.3)) and linearized forms of the trim equations, a relatively simple, closed-form solution (LOTS) can be obtained by using a Lagrange formulation as presented by Bryson and Ho (1975). As will be shown in ensuing numerical examples, the performance degradation for using this simplified approach is negligible for the conditions of cruising flight.

The Lagrange formulation involves forming the Hamiltonian H, which is the sum of the quadratic performance index and the linear equality constraints appended through Lagrange multipliers. For this study, the performance index used is the sum of the induced drag equation and thrust-loss equation, and the linear-equality constraints are the linearized vertical-trim and moment-trim equations. Thus, H is formed as

$$H = C_{D,i} + C_{\mathrm{TL}} + \lambda_{1,\mathrm{VT}} + \lambda_{2,\mathrm{MT}} \tag{2.5.1}$$

where the subscripts VT and MT indicate vertical trim and moment trim, respectively. It should be noted that by properly reformulating the performance index of H, this technique could be applied to other trim optimization problems such as minimizing control deflections or achieving a desired body attitude. The partial derivatives of H with respect to the control variables and the Lagrange multipliers are equivalent to the gradient of the performance index with respect to the control variables while satisfying the trim equations; thus, the sufficient conditions for a minimum are that the partial derivatives of H be equal to zero. For LOTS, the independent design variables are the surface lift coefficients and the thrust deflection angles. Thus, performing the differentiation and setting the derivatives equal to zero give the system of simultaneous linear equations

$$\left.\begin{aligned} \partial H/\partial C_{L,1} &= 0 \\ \partial H/\partial C_{L,2} &= 0 \\ &\vdots \\ \partial H/\partial C_{L,n} &= 0 \\ \partial H/\partial \delta_v &= 0 \\ \partial H/\partial \lambda_1 &= 0 \\ \partial H/\partial \lambda_2 &= 0 \end{aligned}\right\} \tag{2.5.2}$$

where the subscript n denotes the nth lifting surface. When solved, this system yields the linear optimum values of the lift coefficients and thrust-vector angle.

For clarity, solutions for a three-lifting-surface airplane and a two-lifting-surface airplane with thrust vectoring will be illustrated in the following sections. The representative drag and nonlinear trim equations will be presented for these configurations. The trim equations will then be linearized and LOTS will be formed. The effectiveness of the solution will be evaluated by applying LOTS in numerical examples and comparing the results with the results obtained using a nonlinear optimization routine and several ad hoc methods currently in use.

3. LOTS for Three-Lifting-Surface Airplane

Configurations with three lifting surfaces may be attractive for use in general aviation and in transport airplanes because of the capability of yielding minimum trim drag at all center-of-gravity locations. To utilize this capability it is necessary to do some type of longitudinal load-distribution optimization. This section describes the development and validation of a simple method for performing the optimization.

3.1. Development of Solution for Three Lifting Surfaces

For a three-lifting-surface airplane without thrust vectoring, the general trim and drag equations (eqs. (2.1.1), (2.2.1), and (2.3.3)) are applied by setting $n = 3$ and assuming that $\delta_v = 0$. Thus, these equations can be written as follows:

Vertical trim:

$$\sum_{j=1}^{3} \left[C_{L,j} \cos(\alpha - \epsilon_j - \theta) + C_{D,j} \sin(\alpha - \epsilon_j - \theta)\right] \widehat{S}_j + C_T \sin\theta - \overline{W} = 0 \tag{3.1.1}$$

Moment trim:

$$C_{m,o} + \overline{W}\left(\widehat{\ell}_{\text{cg}} \cos\theta + \widehat{z}_{\text{cg}} \sin\theta\right) - C_T \widehat{z}_v - \sum_{j=2}^{3} \left\{C_{L,j}[\cos(\alpha - \epsilon_j)\widehat{\ell}_j + \sin(\alpha - \epsilon_j)\widehat{z}_j] + C_{D,j}[\cos(\alpha - \epsilon_j)\widehat{z}_j - \sin(\alpha - \epsilon_j)\widehat{\ell}_j]\right\} \widehat{S}_j = 0 \tag{3.1.2}$$

Drag:

$$C_{D,i} = \sum_{j=1}^{3}\sum_{k=1}^{3} \frac{\sigma_{jk}}{\pi e_{jk}} \frac{S_1}{b_j b_k} \widehat{S}_j \widehat{S}_k C_{L,j} C_{L,k} \tag{3.1.3}$$

Here, the subscript 1 refers to the wing, 2 to the aft horizontal tail, and 3 to the canard. If the airplane is in cruising flight, it is reasonable to neglect the contributions of drag to the trim equations since the drag forces are generally much less than the lift forces and are usually accompanied by significantly shorter moment arms. The thrust coefficient terms can be neglected for the same reasons. In addition, it is reasonable to assume that the angles θ, ϵ, and α are small, thus allowing sine terms to be approximated by the angle and cosine terms by 1. Using these approximations, the trim equations (eqs. (3.1.1) and (3.1.2)) can be written as

Linearized vertical trim:

$$C_{L,1} + C_{L,2}\widehat{S}_2 + C_{L,3}\widehat{S}_3 - \overline{W} = 0 \tag{3.1.4}$$

Linearized moment trim:

$$C_{m,o} + \overline{W}\widehat{\ell}_{\text{cg}} - C_{L,2}\widehat{\ell}_2\widehat{S}_2 - C_{L,3}\widehat{\ell}_3\widehat{S}_3 = 0 \tag{3.1.5}$$

The trim equations (eqs. (3.1.4) and (3.1.5)) are now linear and can be adjoined with the drag-due-to-lift equation (eq. (3.1.3)) to form the Hamiltonian

$$H = \sum_{j=1}^{3}\sum_{k=1}^{3} \frac{\sigma_{ik}}{\pi e_{jk}} \frac{S_1}{b_j b_k} \widehat{S}_j \widehat{S}_k C_{L,j} C_{L,k} + \lambda_1(C_{L,1} + C_{L,2}\widehat{S}_2 + C_{L,3}\widehat{S}_3 - \overline{W}) + \lambda_2(C_{m,o} + \overline{W}\widehat{\ell}_{\text{cg}} - C_{L,2}\widehat{\ell}_2\widehat{S}_2 - C_{L,3}\widehat{\ell}_3\widehat{S}_3) \tag{3.1.6}$$

Setting the partial derivatives of the Hamiltonian with respect to the independent variables and the Lagrange multipliers ($C_{L,1}$, $C_{L,2}$, $C_{L,3}$, λ_1, and λ_2) equal to zero, and arranging the equations such that the influence-coefficient matrix will be symmetrical, gives

$$\begin{bmatrix} C_{L,1} \\ C_{L,2} \\ C_{L,3} \\ \lambda_1 \\ \lambda_2 \end{bmatrix} = \begin{bmatrix} \frac{2S_1\sigma_{11}}{\pi e_{11} b_1^2} & \frac{2S_2\sigma_{12}}{\pi e_{12} b_1 b_2} & \frac{2S_3\sigma_{13}}{\pi e_{13} b_1 b_3} & 1 & 0 \\ \frac{2S_2\sigma_{12}}{\pi e_{12} b_1 b_2} & \frac{2\widehat{S}_2 S_2\sigma_{22}}{\pi e_{22} b_2^2} & \frac{2S_2 S_3\sigma_{23}}{\pi e_{23} S_1 b_2 b_3} & \widehat{S}_2 & -\widehat{S}_2\widehat{\ell}_2 \\ \frac{2S_3\sigma_{13}}{\pi e_{13} b_1 b_3} & \frac{2S_2 S_3\sigma_{23}}{\pi e_{23} S_1 b_2 b_3} & \frac{2\widehat{S}_3 S_3\sigma_{33}}{\pi e_{33} b_3^2} & \widehat{S}_3 & -\widehat{S}_3\widehat{\ell}_3 \\ 1 & \widehat{S}_2 & \widehat{S}_3 & 0 & 0 \\ 0 & -\widehat{S}_2\widehat{\ell}_2 & -\widehat{S}_3\widehat{\ell} & 0 & 0 \end{bmatrix}^{-1} \begin{bmatrix} 0 \\ 0 \\ 0 \\ \overline{W} \\ C_{m,o} - \overline{W}\widehat{\ell}_{\text{cg}} \end{bmatrix} \tag{3.1.7}$$

The structure of the influence-coefficient matrix provides an interesting insight into the nature of the interactions between surfaces. The influence matrix is composed of only three distinct types of terms. These

three types are area terms, tail-volume terms, and aerodynamic-influence terms. With this idea in mind, the system of equations can be rewritten in the form

$$\begin{bmatrix} C_{L,1} \\ C_{L,2} \\ C_{L,3} \\ \lambda_1 \\ \lambda_2 \end{bmatrix} = \begin{bmatrix} E_{11} & E_{12} & E_{13} & \widehat{S}_1 & 0 \\ E_{12} & E_{22} & E_{23} & \widehat{S}_2 & V_2 \\ E_{13} & E_{23} & E_{33} & \widehat{S}_3 & V_3 \\ \widehat{S}_1 & \widehat{S}_2 & \widehat{S}_3 & 0 & 0 \\ 0 & V_2 & V_3 & 0 & 0 \end{bmatrix}^{-1} \begin{bmatrix} 0 \\ 0 \\ 0 \\ \overline{W} \\ C_{m,o} - \overline{W}\widehat{\ell}_{cg} \end{bmatrix} \tag{3.1.8}$$

The area terms $\widehat{S}_i$ are normalized areas. The tail-volume terms V_i are standard measures of the moment-generating effectiveness of a trim surface. The influence-coefficent terms E_{ij} are measures of the induced drag generated by a surface or the interference drag created between surfaces. It is significant to recognize that the method used to obtain these influence coefficients is at the discretion of the implementer; the terms can be obtained through engineering judgment, analytical means, or experimental data. This flexibility allows LOTS to accommodate the various types of data that may be available during the design and testing processes of an airplane. A relatively simple analytical method for estimating the influence terms is presented in appendix C.

The following numerical example demonstrates the application of LOTS to a three-surface airplane.

3.2. Numerical Example for Three-Lifting-Surface Airplane

A three-view drawing of the example airplane and its specifications are shown in figure 2. The first step toward forming the solution is to determine the Prandtl and efficiency coefficients, σ and e, respectively. This process is detailed in appendix C and the results are as follows:

$$\frac{\sigma_{11}}{e_{11}} = 1.00 \qquad \frac{\sigma_{22}}{e_{22}} = 1.00 \qquad \frac{\sigma_{33}}{e_{33}} = 1.00$$

$$\frac{\sigma_{12}}{e_{12}} = 0.203 \qquad \frac{\sigma_{13}}{e_{13}} = 0.102 \qquad \frac{\sigma_{23}}{e_{23}} = 0.144$$

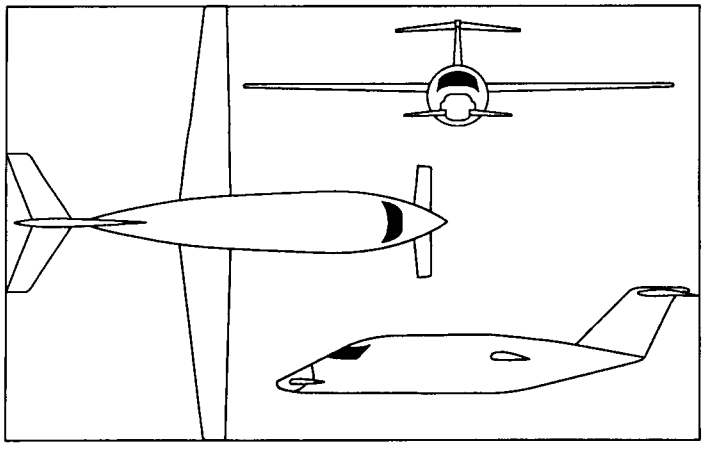

Component	Area, ft^2	Span, ft	Taper ratio	Sweep of 1/4-chord, deg	$\hat{z}$	$\hat{\ell}$
Wing	167	46.5	0.40	0	n/a	n/a
Tail	41.4	13.7	.75	25	1.8	4.32
Canard	22.3	10.6	.75	0	-.62	-6.0
Center of gravity (with s.m. = 10%)					0	-0.15

Figure 2. Three-view drawing and specifications of example three-surface airplane.

In this analysis, the coefficients are assumed constant over the range of flight conditions considered; this condition results in the solution taking a very simple form as will be seen shortly. In practice, these coefficients would vary somewhat as a function of the surface loadings. As these variations are apt to be small over the range of usable cruise lift coefficients, the effect should be minimal. The remaining area and tail-volume terms are easily obtained, thus allowing the system of simultaneous equations (eq. (3.1.8)) to be formed as follows:

$$\begin{bmatrix} C_{L,1} \\ C_{L,2} \\ C_{L,3} \\ \lambda_1 \\ \lambda_2 \end{bmatrix} = \begin{bmatrix} 0.0493 & 0.00840 & 0.00547 & 1 & 0 \\ 0.00840 & 0.0348 & 0.00348 & 0.248 & -1.07 \\ 0.00547 & 0.00348 & 0.0165 & 0.134 & 0.802 \\ 1 & 0.248 & 0.134 & 0 & 0 \\ 0 & -1.07 & 0.802 & 0 & 0 \end{bmatrix}^{-1} \begin{bmatrix} 0 \\ 0 \\ 0 \\ \overline{W} \\ C_{m,o} - \overline{W}\hat{\ell}_{cg} \end{bmatrix} \tag{3.2.1}$$

With all the terms constant in the influence-coefficient matrix constant, the matrix is independent of the flight condition. This independence allows the influence-coefficient matrix to be easily inverted without knowledge of the flight condition, thus resulting in a simple schedule for the optimum values of $C_{L,1}$, $C_{L,2}$ and $C_{L,3}$ with respect to induced trim drag. Thus,

$$C_{L,1} = 0.966\overline{W} - 0.0174(C_{m,o} + \overline{W}\hat{\ell}_{cg}) \tag{3.2.2}$$

$$C_{L,2} = 0.0804\overline{W} + 0.432(C_{m,o} + \overline{W}\hat{\ell}_{cg}) \tag{3.2.3}$$

$$C_{L,3} = 0.107\overline{W} - 0.671(C_{m,o} + \overline{W}\hat{\ell}_{cg}) \tag{3.2.4}$$

Values are shown in figure 3 of $C_{L,1}$, $C_{L,2}$ and $C_{L,3}$ obtained by applying the above control schedule for $C_{m,o} = -0.10$, a static margin that is 10 percent stable, and $\overline{W}$ ranging from 0 to 2.0. The fuselage inclination and control surface deflections required to produce these lift coefficients are shown in figure 4. These positions were obtained through the methods described in appendix A. It is interesting to note that the optimum load for the aft tail is downward. Although this result may not be intuitively obvious, it is also not unexpected; previous research by Sachs (1978), McGeer and Kroo (1983), Kendall (1984), and others has shown that the optimum load distribution may include a negatively loaded trim surface for statically stable two-surface configurations.

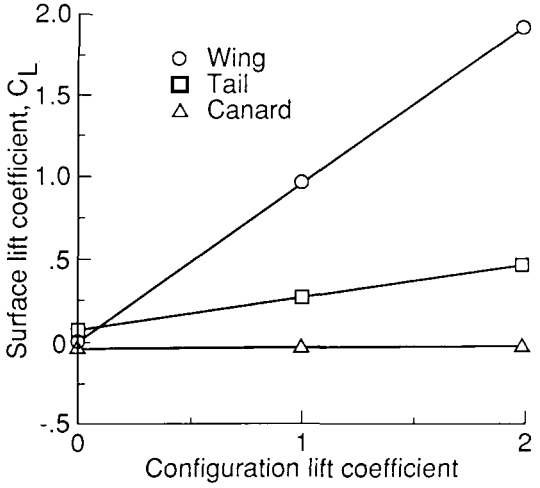

Figure 3. LOTS surface schedule for example three-surface airplane with s.m. = 10 percent stable and $C_{m,o} = -0.10$.

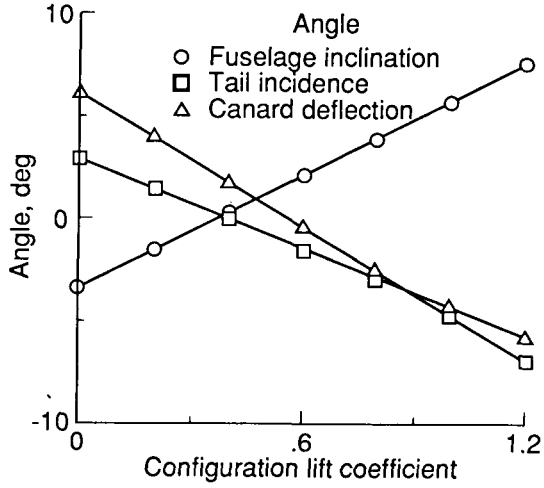

Figure 4. Fuselage inclination, tail incidence, and canard elevator angle versus configuration lift coefficient for example three-surface airplane with s.m. = 10 percent stable and $C_{m,o} = -0.10$.

3.3. Validation of Three-Lifting-Surface Solution

To assess the validity of LOTS as applied to the example three-lifting-surface airplane, a comparison was made of the results obtained from LOTS, a nonlinear optimization routine, and two ad hoc methods suggested

as a simplified means of trimming a three-surface airplane. The nonlinear optimum solution represents the theoretical minimum trim drag and thus provides an ideal baseline by which to assess the performance of the other solutions. The nonlinear optimization routine used is the direct, sequential-search simplex algorithm explained and illustrated by Olsson (1974, 1975). It is extremely reliable and robust in terms of convergence, although it suffers from slow convergence in regions of the independent design variables with low gradients of the performance index. It can be argued that computer resources are much less expensive than the manpower required to supervise other more efficient nonlinear optimization algorithms that need frequent adjustments to ensure proper convergence. Therefore, the robustness and reliability of the simplex algorithm make it highly desirable to use. The first ad hoc distribution considered was to carry no load on the tail. This method is frequently advocated by proponents of canard airplanes who claim that since the aft tail usually contributes to trim by producing a down load, the trim drag will be reduced by unloading it. The second ad hoc method was to carry equal but opposite loads on the tail and canard. This method was suggested by Kendall (1984) as optimum for a three-surface airplane with all surfaces in the same plane and with trim surfaces of equal span.

The vortex-lattice method (VLM) described by Margason and Lamar (1971) was used to evaluate the trim drag of the load distributions as determined by the four trim solutions. The VLM is a relatively sophisticated method of determining the lift and induced drag of a multiplane system in uniform, potential flow. The method consists of modeling the system with a lattice of "horseshoe" vortices, that is, applying boundary conditions to solve for the strengths of the vortices and using these strengths to determine the forces acting on the system. The VLM has been shown to underpredict induced drag slightly; but as long as the paneling scheme is unchanged, this underprediction will be in a manner consistent with exact solutions (Feifel 1976). Thus, the VLM is highly suitable for comparisons of the same system of aerodynamic surfaces at various loadings.

Because LOTS trims the airplane according to linearized trim equations, there is a small amount of trim error present when this distribution is substituted into the nonlinear trim equations. As will be shown, this error is very small and can be neglected for most applications. However, for this study in which the nonlinear trim equations were used to obtain the comparison solutions, it was found that this trim error caused load distributions obtained from LOTS to sometimes have slightly less trim drag than the theoretical minimum. To eliminate this contradiction, it was decided to reduce the trim error of LOTS-obtained distributions to a level comparable to that of the other distributions—the sum of the squares of the vertical-trim and moment-trim errors less than 10^{-9}. This reduction was accomplished by constraining one of the surface lift coefficients to the value obtained from LOTS and using an iterative search technique to reduce the trim error by varying the two remaining surface lift coefficients; in essence, the problem was made determinate around the LOTS distribution. It should be realized that when using nonlinear trim conditions, it is necessary to use an iterative search technique to obtain the two ad hoc solutions as well.

Figures 5 and 6 demonstrate the effects of the trim-error reduction for the three-surface airplane at a static margin of 10 percent stable and with $C_{m,o} = -0.10$. Figure 5 shows the specified lift coefficients before and after the trim-error reduction for the wing and canard. (The tail lift coefficient is held constant.) Figure 6 shows the predicted trim drag before and after the trim-error reduction compared with the results obtained from the nonlinear optimization routine. These results are typical; the trim-error reduction resulted in only a small deviation from the LOTS distributions. The wing and canard lift coefficients usually moved much less than 1 percent from the original value. These very small deviations imply that for most applications, the trim error can be neglected.

As mentioned above, the trim drag obtained through the use of the nonlinear optimization routine is the minimum achievable while satisfying the nonlinear trim conditions and thus can serve as a standard for judging the other solutions. Figures 7, 8, and 9 show the percent of increase in trim drag over the nonlinear optimum solution for the three simplified approaches at various static stability margins and zero-lift pitching moments. Figure 7 represents the airplane at a typical cruise condition with a 10-percent-stable static margin and at $C_{m,o} = -0.10$. Over the range of cruise lift coefficients ($0.3 \leq \overline{W} \leq 0.9$), LOTS is only negligibly less efficient than the nonlinear solutions and is clearly superior to the two alternate procedures. In figure 8 the static stability margin of the airplane is reduced to neutral stability; again, LOTS performs almost as efficiently as the nonlinear solution and much better than the alternate procedures. In figure 9 the static stability margin is returned to 10 percent stable, but the zero-lift pitching moment has been increased to -0.20. The trends of the two previous figures are repeated, and LOTS performs very favorably. These three combinations of pitching moment and static margin serve to demonstrate that although the two ad hoc procedures have regions in which

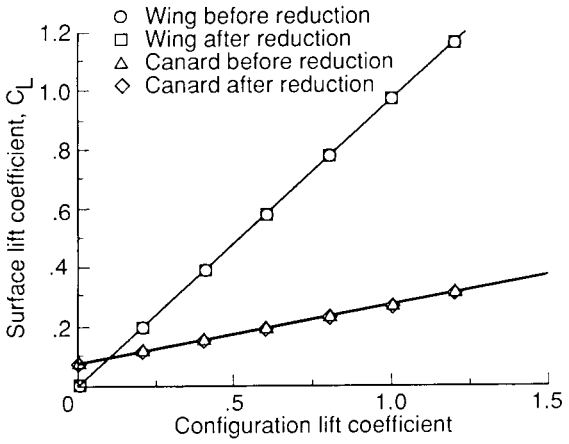

Figure 5. Effect of trim-error reduction on surface lift coefficients.

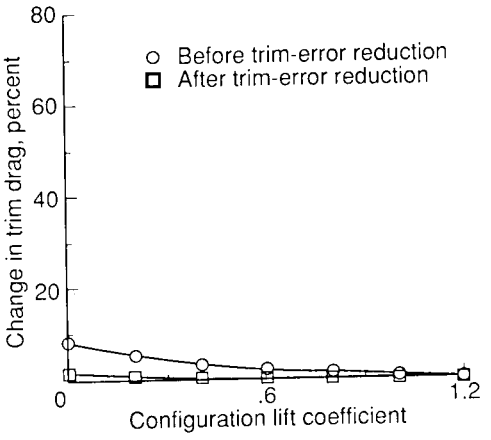

Figure 6. Effect of trim-error reduction on percent of increase in trim drag for example three-surface airplane with s.m. = 10 percent stable and $C_{m,o} = -0.10$.

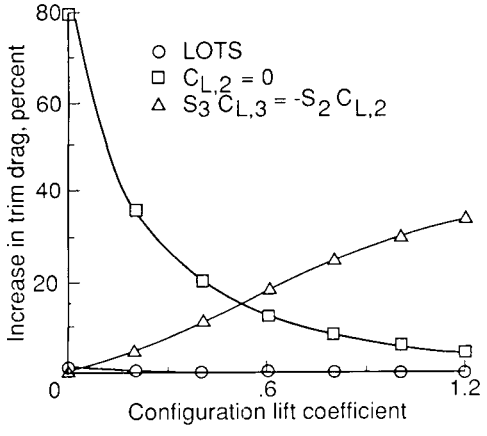

Figure 7. Percent of increase in trim drag over nonlinear optimum solution for example three-surface airplane with s.m. = 10 percent stable and $C_{m,o} = -0.10$.

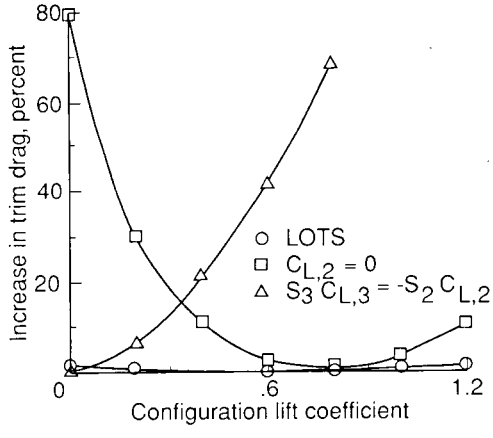

Figure 8. Percent of increase in trim drag over nonlinear optimum solution for example three-surface airplane with s.m. = 0 and $C_{m,o} = -0.10$.

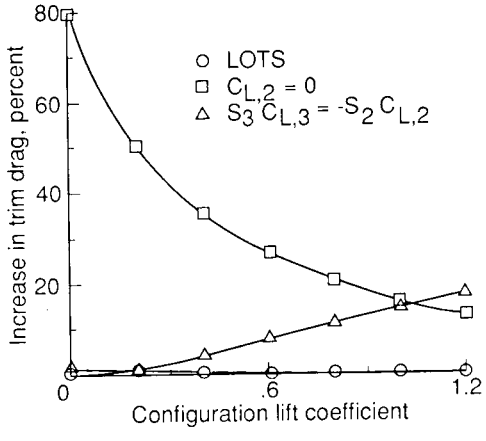

Figure 9. Percent of increase in trim drag over nonlinear optimum solution for example three-surface airplane with s.m. = 10 percent stable and $C_{m,o} = -0.20$.

they may yield near-minimum trim drag, only LOTS achieves this minimum over the range of lift coefficients studied. Furthermore, the optimum methods (LOTS and the nonlinear optimum) can provide trim-drag savings up to 80 percent compared with the ad hoc procedures.

It is difficult to make a direct comparison of the computational time required to obtain LOTS and the nonlinear optimum solution. These times will vary significantly depending on how the solutions are implemented. For the current example, one can get an idea of how great this difference can be by considering the number of calculations required to arrive at the optimum loading. For LOTS, all that needs to be done to obtain the optimum distribution is to substitute the appropriate numbers into equations (3.2.2), (3.2.3), and (3.2.4). By comparison, the nonlinear optimization routine used in this study requires about 400 iterations through the nonlinear trim equations and the VLM drag analysis routine to converge on the optimum distribution. As mentioned before, the direct, sequential-search simplex algorithm used in the nonlinear optimization is not necessarily the fastest such algorithm available, but even more efficient algorithms would still have to perform numerous iterations.

4. LOTS for Two-Lifting-Surface, Thrust-Vectoring Airplane

Although thrust vectoring is usually considered a means for increasing agility or improving short field performance, it can also be used for reducing drag in cruising flight. By taking advantage of the redundant forces and moments that thrust vectoring provides, it is possible to optimize the longitudinal load distribution between the aerodynamic surfaces and the thrust force such that the effective trim drag is less than the trim drag without thrust deflection. By treating the thrust force in a manner similar to the force generated by an aerodynamic surface, the linear optimum trim solution of the previous section has been used to develop a scheduling algorithm that exploits the benefits of thrust vectoring during cruising flight.

4.1. Development of Solution for Two-Lifting-Surface, Thrust-Vectoring Airplane

The first step in developing the method is to write the nonlinear trim and drag equations (eqs. (2.1.1), (2.2.1), and (2.3.3)) as appropriate for a two-surface airplane with thrust vectoring. This is done by setting $n = 2$ in equations (2.1.1), (2.2.1), and (2.3.3) with the following result:

Vertical trim:

$$\sum_{j=1}^{2} \left[(C_{L,j} + k_j C_T \delta_v) \cos(\alpha - \epsilon_j - \theta) + C_{D,j} \sin(\alpha - \epsilon_j - \theta) \right] \widehat{S}_j + C_T \sin(\delta_v + \theta) - \overline{W} = 0 \tag{4.1.1}$$

Moment trim:

$$\begin{aligned} C_{m,o} + \overline{W} \left(\widehat{\ell}_{cg} \cos\theta + \widehat{z}_{cg} \sin\theta \right) - C_T \left(\widehat{\ell}_v \sin\delta_v + \widehat{z}_v \cos\delta_v \right) \\ - \Big\{ (C_{L,2} + k_2 C_T \delta_v) \left[\cos(\alpha - \epsilon_2) \widehat{\ell}_2 + \sin(\alpha - \epsilon_2) \widehat{z}_2 \right] \\ + C_{D,2} \left[\cos(\alpha - \epsilon_2) \widehat{z}_2 - \sin(\alpha - \epsilon_2) \widehat{\ell}_2 \right] \Big\} \widehat{S}_2 = 0 \end{aligned} \tag{4.1.2}$$

Induced drag:

$$C_{D,i} = \sum_{j=1}^{2} \sum_{k=1}^{2} \frac{\sigma_{ik}}{\pi e_{jk}} \frac{S_1}{b_j b_k} \widehat{S}_j \widehat{S}_k (C_{L,j} + k_j \delta_v C_T)(C_{L,k} + k_k \delta_v C_T) \tag{4.1.3}$$

The equations are linearized by making the same approximations regarding cruising flight as made in the three-surface solution regarding small angles and drag. However, unlike the three-surface solution, the thrust terms with components vertical to the body reference line are retained since there is now independent control over its direction and these terms are usually accompanied by long moment arms. These approximations yield the following vertical-trim and moment-trim equations:

Vertical trim:

$$(C_{L,1} + k_1 C_T \delta_v) + (C_{L,2} + k_2 C_T \delta_v) \widehat{S}_2 + C_T(\delta_v + \theta) - \overline{W} = 0 \tag{4.1.4}$$

Moment trim:

$$C_{m,o} - C_T\hat{\ell}_v\delta_v - (C_{L,2} + k_2C_T\delta_v)\hat{\ell}_2\hat{S}_2 + \overline{W}\hat{\ell}_{\text{cg}} = 0 \tag{4.1.5}$$

In level flight α and θ as defined in figure 1 are equal, thus making it possible to approximate the fuselage inclination angle by subtracting the incidence angle between the wing and fuselage (i_1) from the ratio of the wing lift coefficient ($C_{L,1}$) to the linear lift-curve slope ($C_{L_{\alpha,1}}$). That is,

$$\theta = \frac{C_{L,1}}{C_{L_{\alpha,1}}} - i_1 \tag{4.1.6}$$

With this relation, the vertical-trim equation can now be written in the final linearized form as follows:

Vertical trim:

$$C_{L,1}\left(1 + \frac{C_T}{C_{L_{\alpha,1}}}\right) + C_{L,2}\hat{S}_2 + \delta_vC_T(k_1 + k_2\hat{S}_2 + 1) - C_Ti_1 - \overline{W} = 0 \tag{4.1.7}$$

The moment-trim equation is expressed in the necessary form by grouping the thrust-dependent terms:

Moment trim:

$$C_{m,o} - C_T\hat{z}_v - C_{L,2}\hat{\ell}_2\hat{S}_2 - \delta_vC_T\left(\hat{\ell}_v + k_2\hat{\ell}_2\hat{S}_2\right) + \overline{W}\hat{\ell}_{\text{cg}} = 0 \tag{4.1.8}$$

In addition to the induced drag of the aerodynamic surfaces, the cost function must include the thrust-loss term to account for the propulsive force lost because of vectoring for trim. Adding the thrust-loss coefficient to the drag-due-to-lift equation gives the effective drag penalty:

$$P = \sum_{j=1}^{2}\sum_{k=1}^{2}\frac{\sigma_{ik}}{\pi e_{jk}}\frac{S_1}{b_jb_k}\hat{S}_j\hat{S}_k(C_{L,j} + k_j\delta_vC_T)(C_{L,k} + k_k\delta_vC_T) + \mu_{\text{TL}}C_T(1 - \cos\delta_v) \tag{4.1.9}$$

Using equations (4.1.7), (4.1.8), and (4.1.9) to form the Hamiltonian and setting the partial derivatives of H with respect to $C_{L,1}$, $C_{L,2}$, δ_v, λ_1, and λ_2 equal to zero gives a system of five simultaneous equations that can be solved to find the optimum values of $C_{L,1}$, $C_{L,2}$, and δ_v based on the linearized equations. Thus,

$$\begin{bmatrix} C_{L,1} \\ C_{L,2} \\ \delta_vC_T \\ \lambda_1 \\ \lambda_2 \end{bmatrix} = \begin{bmatrix} E_{11} & E_{12} & E_{1v} & G_1 & 0 \\ E_{12} & E_{22} & E_{2v} & G_2 & G_4 \\ E_{1v} & E_{2v} & E_{vv} & G_3 & G_5 \\ G_1 & G_2 & G_3 & 0 & 0 \\ 0 & G_4 & G_5 & 0 & 0 \end{bmatrix}^{-1} \begin{bmatrix} 0 \\ 0 \\ 0 \\ \overline{W} + C_Ti_1 \\ C_T\hat{z}_v - C_{m,o} - \overline{W}\hat{\ell}_{\text{cg}} \end{bmatrix} \tag{4.1.10}$$

where

$$G_1 = 1 + \frac{C_T}{C_{L_{\alpha,1}}}$$

$$G_2 = \widehat{S}_2$$

$$G_3 = k_1 + k_2\widehat{S}_2 + 1$$

$$G_4 = -\widehat{S}_2\widehat{\ell}_2$$

$$G_5 = \left(\widehat{\ell}_v + k_2\widehat{S}_2\widehat{\ell}_2\right)$$

$$E_{11} = \frac{2S_1\sigma_{11}}{\pi e_{11}b_1^2}$$

$$E_{12} = \frac{2S_2\sigma_{12}}{\pi e_{12}b_1b_2}$$

$$E_{1v} = \frac{2}{\pi b_1}\left(\frac{\sigma_{11}S_1k_1}{e_{11}b_1} + \frac{\sigma_{12}S_2k_2}{e_{12}b_2}\right)$$

$$E_{22} = \frac{2S_2\sigma_{22}\widehat{S}_2}{\pi e_{22}b_2^2}$$

$$E_{2v} = \frac{2S_2}{\pi b_2}\left(\frac{\sigma_{12}k_1}{e_{12}b_1} + \frac{\sigma_{22}S_2k_2}{e_{22}b_2S_1}\right)$$

$$E_{vv} = \frac{2}{\pi}\left(\frac{\sigma_{11}S_1k_1^2}{e_{11}b_1^2} + \frac{2\sigma_{12}S_2k_1k_2}{e_{12}b_1b_2} + \frac{\sigma_{22}S_2k_2^2\widehat{S}_2}{e_{22}b_2^2}\right) + \frac{\mu_{\mathrm{TL}}}{C_T}$$

Unlike the three-surface solution (eq. (4.1.7)), the influence-coefficient matrix for this thrust-vectoring-equipped airplane contains the thrust coefficient. Because the thrust coefficient depends on the flight condition, the influence matrix is also dependent on the flight condition. This dependence makes it inconvenient to invert the influence matrix (as was shown for the three-surface solution) until the value of the thrust coefficient has been obtained or estimated.

The following example demonstrates LOTS for a typical two-surface airplane with thrust vectoring.

4.2. Numerical Example for Two-Lifting-Surface, Thrust-Vectoring Airplane

A three-view drawing of the example airplane and its relevant specifications are shown in figure 10. Estimates of the aerodynamic efficiency and influence terms were obtained using the method described in appendix C and are given as follows:

$$\frac{\sigma_{11}}{e_{11}} = 1.00 \qquad \frac{\sigma_{22}}{e_{22}} = 1.00 \qquad \frac{\sigma_{12}}{e_{12}} = 0.116$$

The lift-curve slope of the wing was estimated using VLM analysis to be 3.46 per radian. In addition to the aerodynamic influence terms and lift-curve slope, estimates need to be obtained of the thrust/aerodynamic interaction terms (k_i and μ_{TL}). Analytical methods for estimating these terms are unknown to the authors, and little applicable experimental data have been published. To simplify the demonstration of LOTS, the values of k_1 and k_2 used in this example are zero. For the example airplane where the separation between the wing and the jet nozzle is significant and little interaction is expected, the actual value of k_1 is probably near zero. However, the tail surface of this airplane is located very near the jet nozzle and significant interaction may occur, thus making the actual value of k_2 likely to be nonzero. To bound the effects of thrust, recovery values of 0, 0.5, and 1.0 were used for μ_{TL}. Experimental data from Lowry et al. (1957) indicate that a value of μ_{TL} between 0.5 and 0 may be expected in practice. With all the terms in the influence matrix in hand, the

solution can be written as

$$\begin{bmatrix} C_{L,1} \\ C_{L,2} \\ C_T\delta_v \\ \lambda_1 \\ \lambda_2 \end{bmatrix} = \begin{bmatrix} 0.180 & 0.0371 & 0 & 1.0+0.289C_T & 0 \\ 0.0371 & 0.0570 & 0 & 0.220 & -0.346 \\ 0 & 0 & \mu_{\mathrm{TL}}/C_T & 1.0 & -1.96 \\ 1.0+0.289C_T & 0.220 & 1.0 & 0 & 0 \\ 0 & -0.346 & -1.96C_T & 0 & 0 \end{bmatrix}^{-1} \begin{bmatrix} 0 \\ 0 \\ 0 \\ \overline{W} \\ C_{m,o} - \overline{W}\hat{\ell}_{\mathrm{cg}} \end{bmatrix} \tag{4.2.1}$$

As pointed out in the previous section, the presence of C_T in the influence-coefficient matrix of equation (4.2.1) makes the inversion of the influence matrix impractical until C_T has been estimated or measured for a given throttle setting and flight condition. An estimate of C_T can be obtained by using standard drag-estimation techniques and assuming that $C_T = C_D$. The values of $C_{L,1}$, $C_{L,2}$, and δ_v obtained from the above solution are shown in figures 11 and 12 for $C_{m,o} = -0.10$, a static margin of 3 percent stable, $\mu_{\mathrm{TL}} = 0.5$, and a Mach number ranging from 0.3 to 0.9.

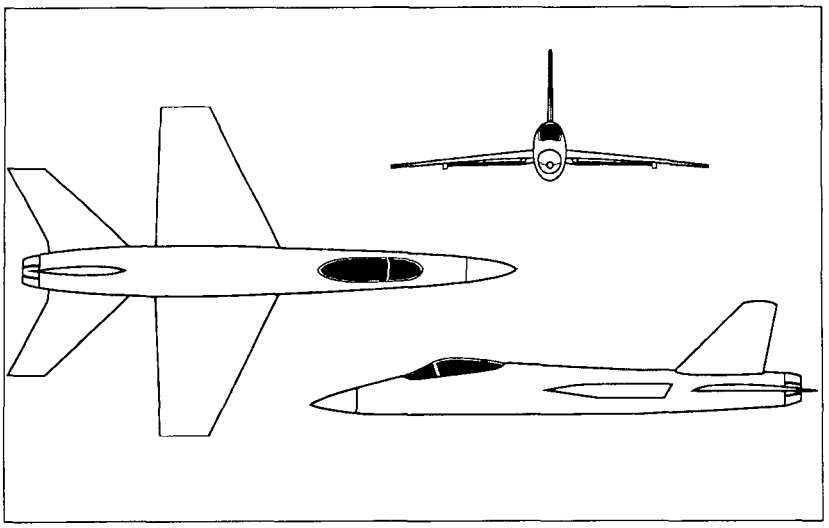

Component	Area, ft^2	Span, ft	Taper ratio	Sweep of 1/4-chord, deg	$\hat{z}$	$\hat{\ell}$
Wing	400	37.5	0.35	20	n/a	n/a
Tail	88.1	14.7	.46	40	0.05	1.4
Nozzle	n/a	n/a	n/a	n/a	0	1.8
Center of gravity (with s.m. = 3%)					0	-0.056

Figure 10. Three-view drawing and specifications of example two-surface, thrust-vectoring airplane.

4.3. Validation of Two-Lifting-Surface, Thrust-Vectoring Solution

To assess the validity of LOTS as applied to the example two-lifting-surface, thrust-vectoring airplane, a study similar to the one used to validate the three-surface solution was conducted. An investigation was made of the results obtained from LOTS, a nonlinear optimization routine, and trimming the airplane without using the thrust-vectoring capability ($\delta_v = 0$). As in the previous section, the nonlinear optimization routine used is the direct, sequential-search simplex algorithm described by Olsson (1974, 1975), and the VLM was used to evaluate the effective trim drag of the various load distributions. It should be noted that the VLM routine used in this comparison was incapable of estimating the effects of supercirculation. Consequently, any changes in aerodynamic lift due to thrust vectoring were not modeled and thrust recovery was included simply by selecting, a priori, a percentage of thrust that was recovered. A trim-error-reduction routine, identical to the

one described in the previous section, was included in the implementation of the LOTS solution. As before, this trim-error reduction had only a small effect on the LOTS distributions.

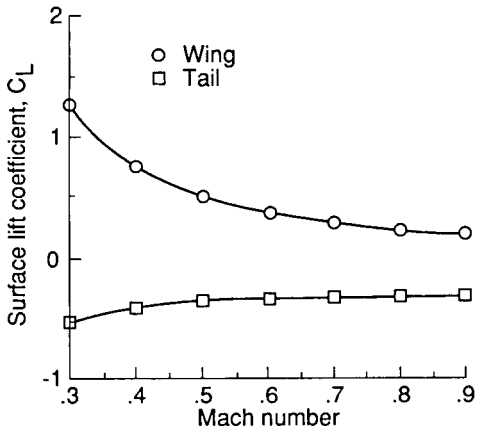

Figure 11. LOTS surface schedule for example two-surface, thrust-vectoring airplane with $\mu_{TL} = 0.5$ for wing and tail.

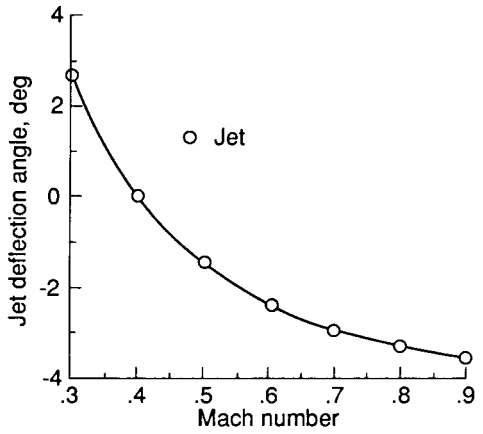

Figure 12. LOTS surface schedule for example two-surface, thrust-vectoring airplane with $\mu_{TL} = 0.5$ for jet.

As was done in the previous section, the distributions obtained from the nonlinear optimization routine, having the lowest achievable effective trim drag, were used as a baseline to evaluate the other techniques. Figures 13, 14, and 15 show the percent of increase in effective trim drag compared with the nonlinear optimum solution for LOTS when trimming while holding δ_v to zero with μ_{TL} equal to 0.0, 0.5, and 1.0, respectively. As can be seen from the figures, LOTS yields nearly the same results as the nonlinear optimum solution over the range of flight conditions and μ_{TL} studied. For a Mach number M from approximately 0.4 to 0.5, neither of the optimum methods results in a significant trim-drag reduction compared with trimming without using the thrust vectoring. This absence of savings is because the optimum thrust deflection angle in this Mach number range is nearly zero, and hence little reduction is possible.

It is interesting to note the sensitivity of the effective trim drag to the amount of thrust recovery. When no thrust is lost ($\mu_{TL} = 0$), the optimum solutions predict trim-drag reductions of over 70 percent compared with holding δ_v equal to zero for the typical cruise Mach number region (0.8 to 0.9). However, when half the deflected thrust component is lost ($\mu_{TL} = 0.5$), the reduction in effective trim drag drops to around 5 percent. When none of the deflected thrust is recovered ($\mu_{TL} = 1.0$), the reduction is only 2 percent. It appears that to use thrust vectoring as a viable means of reducing trim drag, the design should recover a high percentage of the deflected thrust.

5. Other Potential Applications of LOTS

The simplicity, speed, and closed-form nature of LOTS also make it suited for applications in airplane testing and operations.

5.1. Experimental Testing

Frequently, the procedure used for testing models in a wind tunnel is to fix the control effectors while sweeping through a range of angle of attack or sideslip. For conventional airplanes (i.e., two lifting surfaces and no thrust vectoring), this procedure will generally result in the collection of data from which the characteristics of the trimmed configuration can be easily and accurately interpolated. However, because of the redundancy of forces and moments, this technique may not result in such data for airplanes with multiple lifting surfaces or propulsive control effectors. In order to collect data that reflect the optimum trimmed aerodynamics of the model, it is necessary to set the surfaces and effectors in the optimum positions for a given test condition. LOTS provides a simple means of calculating the optimum lift coefficients of the surfaces, and the required surface positions can be estimated using the methods provided in appendix B. Ideally, this entire scheduling process would be automated on a programmable calculator or personal computer, thus placing little additional burden on the experimenter.

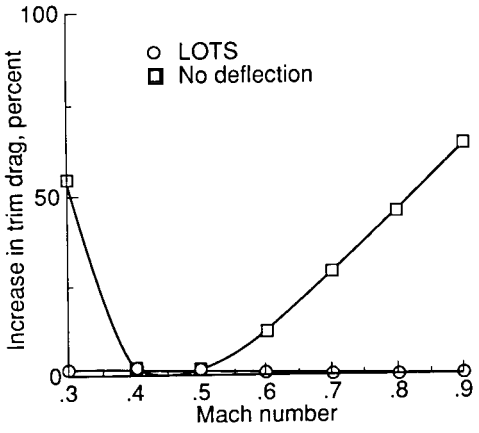

Figure 13. Percent of increase in effective trim drag over nonlinear optimum solution for example two-surface, thrust-vectoring airplane with $\mu_{TL} = 0$.

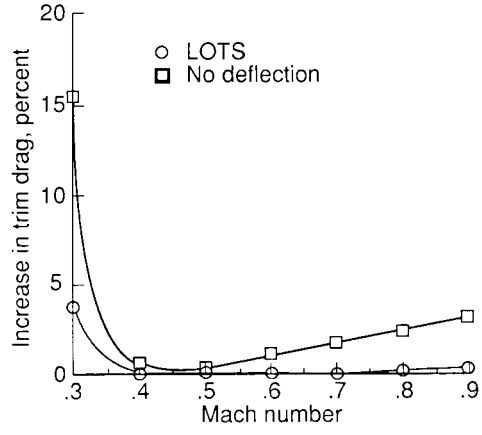

Figure 14. Percent of increase in effective trim drag over nonlinear optimum solution for example two-surface, thrust-vectoring airplane with $\mu_{TL} = 0.5$.

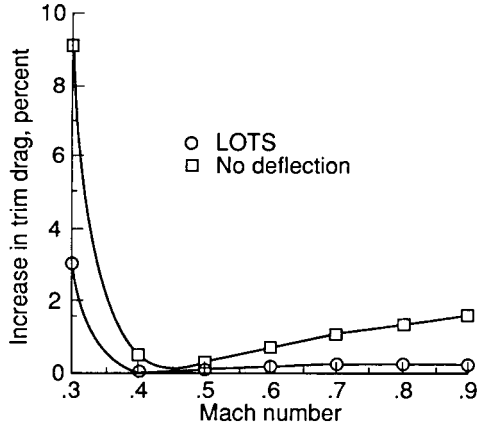

Figure 15. Percent of increase in effective trim drag over nonlinear optimum solution for example two-surface, thrust-vectoring airplane with $\mu_{TL} = 1.0$.

5.2. In-Flight Operations

The speed with which the minimum trim-drag lift distribution can be found using LOTS could make in-flight trim optimization a possibility. Once the solution has been set up for a given configuration, all that is needed to determine the optimum distribution is the current flight condition. These data could be obtained from the air data system, the throttle position, and an estimate of the gross weight and center-of-gravity location. The solution of the set of simultaneous equations in real time should be well within the capability of currently available flight computers. The entire process could be implemented as part of the control system, thus making the optimization process transparent to the flight crew.

6. Concluding Remarks

The research described in this paper investigates a closed-form trim solution yielding minimum trim drag. The solution known as the linear optimum trim solution (LOTS) provides designers a technique to trim, with minimum trim drag, redundantly controlled airplanes in the conceptual and preliminary design stages with rather straightforward analytical formulas. Potential applications in experimental testing and in-flight operations are also briefly discussed.

The benefits of LOTS and the optimum longitudinal load distribution to produce minimum drag in general are investigated by trimming vortex-lattice representations of a three-surface airplane and a two-surface, thrust-vectoring airplane using LOTS, a nonlinear optimization routine, and ad hoc techniques. This investigation shows that the performance of LOTS is insignificantly less than the nonlinear optimum over the range of conditions studied. Furthermore, the optimum trim solutions have been shown to provide trim-drag reductions up to 80 percent compared with the ad hoc techniques for the example three-surface airplane and 70 percent for the thrust-vectoring airplane. These trim-drag savings are on the order of 0.5 to 1.0 percent of the total airplane drag.

NASA Langley Research Center
Hampton, VA 23665-5225
March 1, 1989

Appendix A

Surface Deflections

After the optimum longitudinal load distribution has been determined, it may be necessary to estimate the control surface deflections and incidence angles required to generate the specified lifts. There are many methods available to accomplish this task and one is free to select a method consistent with his objectives. The method presented in this appendix was chosen for its relative simplicity. Its use should be restricted to lift coefficients where no significant flow separation is expected.

The lift coefficient of an aerodynamic surface (Datcom 1978) can be expressed as

$$C_L = C_{L_\alpha}(\alpha + \epsilon + i - \Delta\alpha_0 L) \tag{A1}$$

where

C_{L_α} lift-curve slope

i incidence angle between zero-lift line and body reference line

α angle of attack of body reference line

$\Delta\alpha_0 L$ change in i due to deflection of simple hinged control flap

ϵ local downwash angle

By estimating the appropriate dependent variables and then choosing the proper value for the independent variable, equation (A1) can be used for scheduling most conventional surfaces. For instance, if the incidence of the main wing is fixed and if the optimum position of any camber-changing devices on the wing has been determined, α will be the independent variable used to achieve the desired wing lift coefficient. For trim surfaces with variable incidence, i will be the independent variable used to obtain the desired coefficient; and for surfaces with a hinged control flap, $\Delta\alpha_0 L$ will be used. Procedures for estimating the dependent terms are as follows:

The term C_{L_α} can be approximated by using the following relation from Nicolai (1975):

$$C_{L_\alpha} = \frac{2\pi A}{2 + \left[4 + A^2\beta^2\left(1 + \frac{\tan^2 \Lambda_{t/c}}{\beta^2}\right)\right]^{1/2}}$$

where

A aspect ratio

β $= \sqrt{1 - M_\infty^2}$

$\Lambda_{t/c}$ sweep of maximum thickness line

The average downwash angle ϵ at a surface can be found using the following methods (Datcom 1978). The term ϵ_2, which represents the downwash at the aft tail due to the wing (the canard contribution is negligible), is given as

$$\epsilon_2 = \frac{\partial \epsilon_1}{\partial \alpha}\alpha_{\text{eff},1}$$

where

$$\frac{\partial \epsilon_1}{\partial \alpha} = -4.44 \left[K_A K_{\text{TR}} K_H (\cos \Lambda_{1/4})^{1/2} \right]^{1.19}$$

$$K_A = \frac{1}{A} - \frac{1}{1 + A^{1.7}}$$

$$K_{\text{TR}} = \frac{10 - 3\text{TR}}{7}$$

$$K_H = \frac{1 - |\frac{h_t}{b}|}{\left(\frac{2\ell_t}{b}\right)^{1/3}}$$

and

h_t vertical separation of wing and aft tail

ℓ_t horizontal separation of wing and aft tail

TR taper ratio of wing

α_{eff} $= \alpha + \epsilon + i - \Delta\alpha_0 L_1$

$\Lambda_{1/4}$ sweep of 1/4-chord line

The method above can be adapted to estimate the downwash at the wing ϵ_1 by treating the wing as the aft tail, the canard as the wing, and calculating $\partial\epsilon_3/\partial\alpha$ as

$$\frac{\partial \epsilon_1}{\partial \alpha} = -4.44 \frac{S_c}{S_w} \left[K_A K_{\text{TR}} K_H \left(\cos \Lambda_{1/4} \right)^{1/2} \right]^{1.19}$$

where S_c/S_w is the canard area divided by the wing area.

To estimate the upwash produced at the canard by the wing, the following method by Perkins and Hage (1949) can be used. The effect of the wing on the canard ϵ_3 is given as

$$\epsilon_3 = \frac{\partial \epsilon_2}{\partial \alpha} \alpha_{\text{eff},1}$$

where

$$\frac{\partial \epsilon_2}{\partial \alpha} = 0.9(0.722)^{\left(\frac{5\ell_w}{c} - 2\right)}$$

ℓ_w is the horizontal separation of the canard and wing, and c is the length of the mean aerodynamic chord.

Because of the coupling of $\alpha_{\text{eff},1}$ and $\alpha_{\text{eff},3}$, several iterations of the scheduling process may be required to converge on a satisfactory solution.

The term $\Delta\alpha_0 L$ can be approximated by using the following relations from Datcom (1978):

$$\Delta\alpha_0 L = -C_{l_\alpha} \frac{1}{C_{L_\alpha}} \delta_f K'$$

where

C_{l_δ} lift effectiveness of plain trailing-edge flap, $C_1 + C_2 \frac{C_f}{C} + C_3 \left(\frac{C_f}{C}\right)^2$

C_f/C = Flap chord/Total wing chord

C_1 $= 1.242 - \frac{0.5991t}{c}$

C_2 $= 12.98 + \frac{12.44t}{c}$

C_3 $= -10.53 - \frac{0.6497t}{c}$

K' flap-effectiveness factor at large deflections

t/c = Wing thickness/Wing chord

δ_f flap deflection, rad

and

$$K' = K_1 + K_2\delta_f + K_3\delta_f^2 + K_4\delta_f^3$$

where

$$K_1 = 1.011 + 0.1740\ \frac{C_f}{C}$$

$$K_2 = 0.002053 - 0.02069\ \frac{C_f}{C}$$

$$K_3 = 0.0004845 + 0.00002479\ \frac{C_f}{C}$$

$$K_4 = 5.688 \times 10^{-6} - 1.217 \times 10^{-7}\ \frac{C_f}{C}$$

Appendix B

Analytical Approximations for Effects of Supercirculation

Experimental studies have shown that the deflected jet of a thrust-vectoring airplane can significantly alter the flow field about the airplane. The name given to this alteration is supercirculation. Supercirculation has two primary effects—induced lift and thrust recovery—as clarified in the subsequent discussion.

Induced Lift

Induced lift is a change in the lift produced by the aerodynamic surfaces of an airplane due to the presence of thrust vectoring. The deflected jet acts in a manner similar to a jet flap, that is, altering the circulation about the surfaces and thus altering the amount of lift produced. The induced lift coefficient $C_{L,\Gamma}$ was modeled as a function of thrust coefficient C_T and thrust deflection angle δ_v. Figure B1 shows thrust deflection angle versus normalized C_T (Lowry et al. 1957). This figure indicates that $C_{L,\Gamma}$ can be modeled as

$$C_{L,\Gamma} = k\delta_v C_T$$

where k is a constant depending on surface and nozzle geometry factors.

Thrust Recovery

Thrust recovery is the fraction of deflected thrust that is eventually recovered to provide an effective thrust component. The term "thrust recovery" is somewhat misleading; the process that actually takes place is a reduction in induced drag. This reduction is due primarily to an upwash field created in front of the surfaces of the airplane by the deflected jet. Figure B2 (Capone 1974) shows the effect of thrust deflection on the drag characteristics of an airfoil. The figure shows that increasing the thrust deflection angle decreases the drag coefficient. With the process of thrust recovery in mind, the model for effective thrust coefficient becomes

$$C_{T,e} = C_T \cos\delta_v + \eta_{\mathrm{TR}} C_T (1 - \cos\delta_v)$$

where η_{TR} is the fraction of thrust recovered.

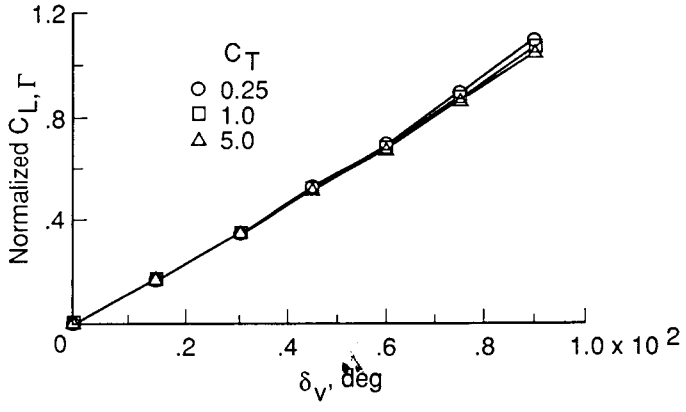

Figure B1. Supercirculation lift model.

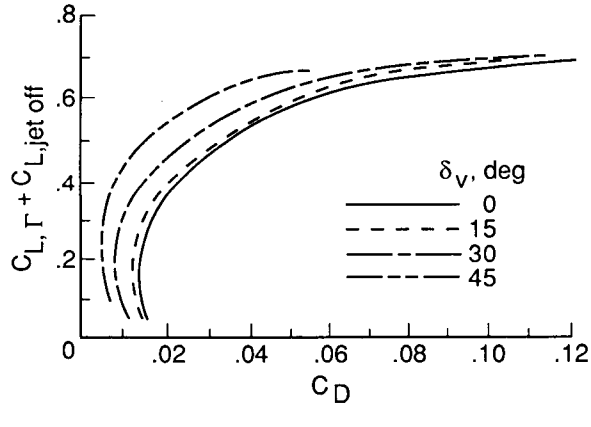

Figure B2. Effect of nozzle deflection on drag characteristics. $M = 0.7$; $C_T = 0.125$.

Since in this analysis we are interested in the lost thrust and not in the effective thrust, we form the relation for the thrust-loss coefficient as

$$C_{\mathrm{TL}} = C_T - C_{T,e} = C_T(1 - \cos\delta_v - \eta_{\mathrm{TR}} + \eta_{\mathrm{TR}}\cos\delta_v) = \mu_{\mathrm{TL}} C_T (1 - \cos\delta_v)$$

where $\mu_{\mathrm{TL}} = 1 - \eta_{\mathrm{TR}}$ and is the fraction of thrust loss. Experimental data presented by Lowry et al. (1957) indicate that between 50 to 100 percent of the deflected thrust can be recovered at low-to-moderate thrust deflection angles ($< 20°$); hence, μ_{TL} will generally have a value between 0 and 0.5.

Appendix C

A Technique for Estimating e and σ

Before the linear optimum trim solution can be implemented, estimates of the efficiency factors e and the Prandtl coefficients σ must be obtained. The methods used to obtain these coefficients are independent of the linear optimum solution—the implementer is free to use any applicable method, be it analytical or experimental. The following equations provide a simple analytical means for obtaining these coefficients.

The e_{jj} terms can be estimated using figure C1 to obtain the vortex-induced drag factor δ for surface i (Torenbeek 1982) and the relation $e = 1/(1+\delta)$.

According to Butler (1983), the e_{jk} terms can be written as

$$e_{jk} = e_{ii}^{1/2} \times e_{jj}^{1/2}$$

and the σ_{jk} terms can be estimated as

$$\sigma_{jk} = \frac{b_s}{b_w}\left\{1 - \frac{2g}{b_w}\left[1 + \left(\frac{2g}{b_w}\right)^{-1/2}\right]\right\} - \frac{b_s}{b_w}\left[0.75\left(\frac{g}{b_w}\right)^{1/2} - \frac{g}{b_w}\right]$$

where

b_s smaller of two spans

b_w larger of two spans

g vertical gap between surfaces

Inspection of the above relation reveals that $\sigma_{jk} = \sigma_{kj}$ and $\sigma_{jj} = 1$.

Rather than using the above equations to determine the efficiency factors and Prandtl coefficients of the example airplane in sections 3 and 4, the VLM described in section 3 was utilized. By using the VLM to determine both the influence coefficients and the trim drag of the configurations, a potential source of disagreement was eliminated. The results from the VLM were compared with the results obtained from the equations above and were found to be nearly identical. The application of the VLM to find the influence coefficients of the three-surface airplane is as follows. By analyzing the surfaces of the example airplane individually and in pairs, estimates of the aerodynamic influence terms were obtained directly.

From the quadratic model of drag due to lift (eq. (3.1.3)),

$$\frac{C_{D,i,jj}}{C_{L,jj}^2} = \frac{\sigma_{jj}}{\pi e_{jj}} \frac{S_i}{b_j^2} \widehat{S}_j$$

and

$$\frac{C_{D,i,jk}}{C_{L,j} C_{L,k}} = \frac{2\sigma_{jk}}{\pi e_{jk}} \frac{S_j S_k}{b_j b_k} \qquad (j \neq k)$$

Hence, the E_{11} term of the influence matrix in equation (3.1.8) can be found by

$$E_{11} = \frac{C_{D,i,11}}{C_{L,11}^2} \times 2$$

where $C_{D,i,11}$ is the induced drag coefficient estimated by the VLM for the isolated wing generating the lift coefficient $C_{L,11}$. Similarly,

$$E_{22} = \frac{C_{D,i,22}}{C_{L,22}^2} \times 2 \times \widehat{S}_2$$

and

$$E_{33} = \frac{C_{D,i,33}}{C_{L,33}^2} \times 2 \times \widehat{S}_3$$

The E_{jk} terms (where $j \neq k$) were found by taking the difference in induced drag between the surfaces tested in pairs and those tested individually and using the relation

$$E_{jk} = \frac{\Delta C_{D,i,jk}}{C_{L,j} C_{L,k}}$$

The influence coefficients were determined in an identical manner for the example thrust-vectoring airplane.

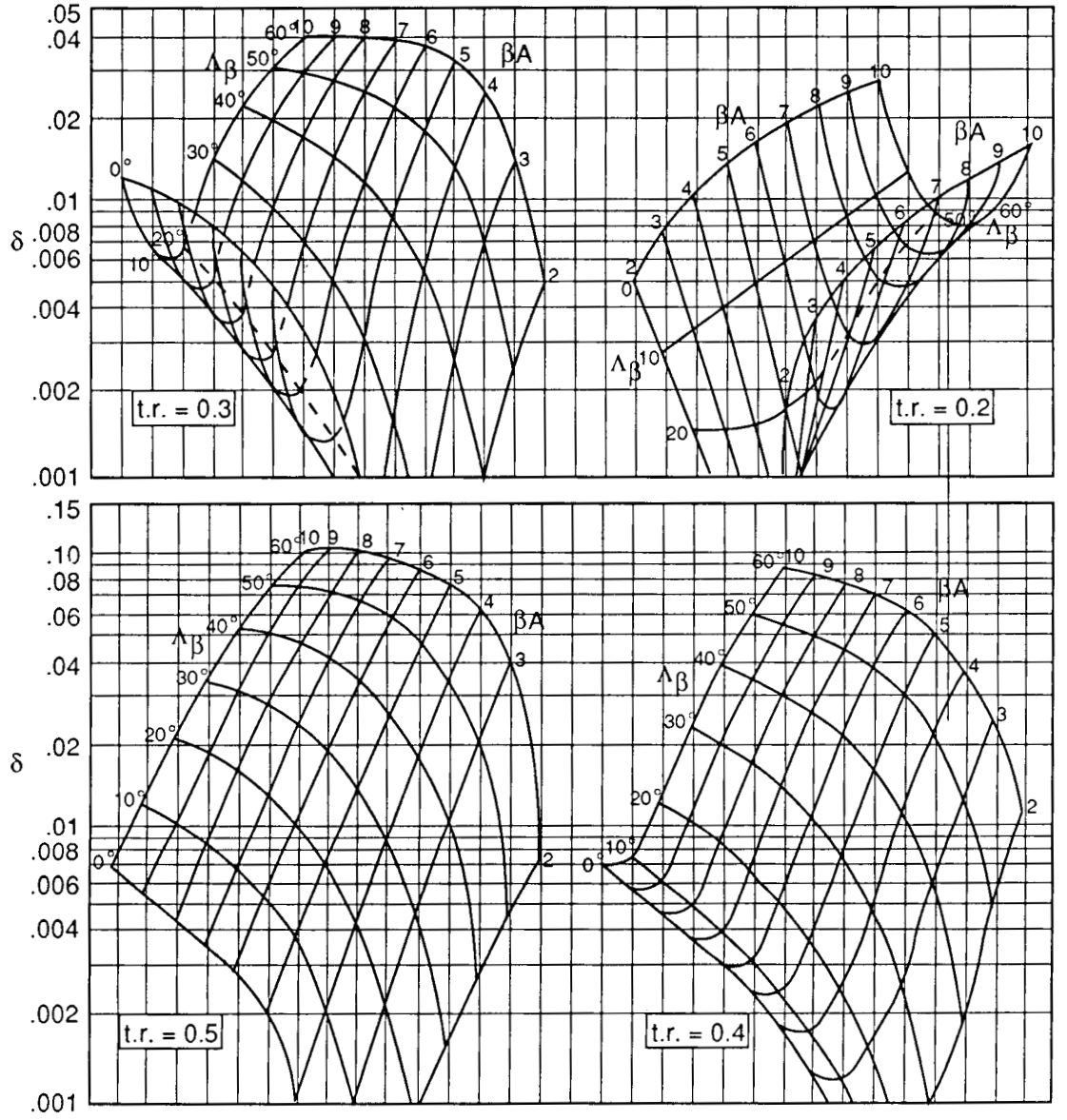

A aspect ratio
t.r. surface taper ratio
β Prandtl's compressibility correction, $\sqrt{1 - M^2}$
Λ sweep angle of surface quarter-chord line
Λ_β corrected sweep angle ($\tan \Lambda_\beta = \tan \Lambda_{1/4}/\beta$), deg

Figure C1. The vortex-induced drag factor δ taken from page 494 of Torenbeek (1982).

References

Bryson, Arthur E., Jr.; and Ho, Yu-Chi: *Applied Optimal Control, Revised printing.* Hemisphere Publ. Corp., c.1975.

Butler, G. F.: An Analytical Study of the Induced Drag of Canard-Wing-Tail Aircraft Configurations With Various Levels of Static Stability. *Aeronaut. J.*, vol. 87, no. 868, Oct. 1983, pp. 293–300.

Capone, Francis J.: Supercirculation Effects Induced by Vectoring a Partial-Span Rectangular Jet. AIAA Paper No. 74-971, Aug. 1974.

Capone, Francis J.; and Reubush, David E.: *Effects of Varying Podded Nacelle-Nozzle Installations on Transonic Aeropropulsive Characteristics of a Supersonic Fighter Aircraft.* NASA TP-2120, 1983.

Durand, William Frederick, ed.: *Aerodynamic Theory, Volume IV.* Julius Springer (Berlin), 1935.

Feifel, Winfried M.: Optimization and Design of Three-Dimensional Aerodynamic Configurations of Arbitrary Shape by a Vortex Lattice Method. *Vortex-Lattice Utilization*, NASA SP-405, 1976, pp. 71–88.

Kendall, Eric R.: The Minimum Induced Drag, Longitudinal Trim and Static Longitudinal Stability of Two-Surface and Three-Surface Airplanes. AIAA-84-2164, Aug. 1984.

Lowry, John G.; Riebe, John M.; and Campbell, John P.: The Jet-Augmented Flap. Preprint No. 715, S.M.F. Fund Paper, Inst. of Aeronautical Sciences, Jan. 1957.

Margason, Richard J.; and Lamar, John E.: *Vortex-Lattice FORTRAN Program for Estimating Subsonic Aerodynamic Characteristics of Complex Planforms.* NASA TN D-6142, 1971.

McGeer, Tad; and Kroo, Ilan: A Fundamental Comparison of Canard and Conventional Configurations. *J. Aircr.*, vol. 20, no. 11, Nov. 1983, pp. 983–992.

Nicolai, Leland M.: *Fundamentals of Aircraft Design.* School of Engineering, Univ. of Dayton, Dayton, Ohio, c.1975.

Olsson, D. M.: A Sequential Simplex Program for Solving Minimization Problems. *J. Qual. Technol.*, vol. 6, no. 1, Jan. 1974, pp. 53–57.

Olsson, Donald M.; and Nelson, Lloyd S.: The Nelder-Mead Simplex Procedure for Function Minimization. *Technometrics*, vol. 17, no. 1, Feb. 1975, pp. 45–51.

Perkins, Courtland D.; and Hage, Robert E.: *Airplane Performance Stability and Control.* John Wiley & Sons, Inc., c.1949.

Rokhsaz, Kamran; and Selberg, Bruce P.: Analytical Study of Three-Surface Lifting Systems. *General Aviation Aircraft Aerodynamics*, SP-621, Soc. of Automotive Engineers, Inc., 1985, pp. 85–94. (Available as SAE Paper 850866.)

Sachs, Gottfried: Minimum Trimmed Drag and Optimum c.g. Position. *J. Aircr.*, vol. 15, no. 8, Aug. 1978, pp. 456–459.

Torenbeek, Egbert: *Synthesis of Subsonic Airplane Design.* Delft Univ. Press and Martinus Nijhoff Publ. (Holland), c.1982.

USAF Stability and Control Datcom. Contracts AF33(616)-6460 and F33615-76-C-3061, McDonnell Douglas Corp., Oct. 1960. (Revis. Apr. 1978.)

NASA
National Aeronautics and Space Administration

Report Documentation Page

1. Report No.	2. Government Accession No.	3. Recipient's Catalog No.
NASA TP-2907		

4. Title and Subtitle	5. Report Date
A Closed-Form Trim Solution Yielding Minimum Trim Drag for Airplanes With Multiple Longitudinal-Control Effectors	May 1989
	6. Performing Organization Code
7. Author(s)	8. Performing Organization Report No.
Kenneth H. Goodrich, Steven M. Sliwa, and Frederick J. Lallman	L-16484
9. Performing Organization Name and Address	10. Work Unit No.
NASA Langley Research Center Hampton, VA 23665-5225	505-66-01-02
	11. Contract or Grant No.
12. Sponsoring Agency Name and Address	13. Type of Report and Period Covered
National Aeronautics and Space Administration Washington, DC 20546-0001	Technical Paper
	14. Sponsoring Agency Code

15. Supplementary Notes

16. Abstract

Airplane designs are currently being proposed with a multitude of lifting and control devices. Because of the redundancy in ways to generate moments and forces, there are a variety of strategies for trimming such airplanes. A linear optimum trim solution (LOTS) is derived using a Lagrange formulation. LOTS enables the rapid calculation of the longitudinal load distribution resulting in the minimum trim drag in level, steady state flight for airplanes with a mixture of three or more aerodynamic surfaces and propulsive control effectors. Comparisons of the trim drags obtained using LOTS, a direct, constrained optimization method, and several ad hoc methods are presented for vortex-lattice representations of a three-surface airplane and a two-surface airplane with thrust vectoring. These comparisons show that LOTS accurately predicts the results obtained from the nonlinear optimization and that the optimum methods result in trim-drag reductions up to 80 percent compared with the ad hoc methods.

17. Key Words (Suggested by Authors(s))
Three-surface configurations
Thrust vectoring
Redundant control
Trim optimization
Design of airplanes

18. Distribution Statement
Unclassified—Unlimited

Subject Category 08

19. Security Classif. (of this report)	20. Security Classif. (of this page)	21. No. of Pages	22. Price
Unclassified	Unclassified	29	A03